

REPORT DOCUMENTATION PAGE

Form Approved  
OMB No. 0704-0188

Public reporting burden for this collection of information is estimated to average 1 hour per response, including the time for reviewing instructions, searching existing data sources, gathering and maintaining the data needed, and completing and reviewing the collection of information. Send comments regarding this burden estimate or any other aspect of this collection of information, including suggestions for reducing this burden, to Washington Headquarters Service, Directorate for Information Operations and Reports, 1215 Jefferson Davis Highway, Suite 1204, Arlington, VA 22202-4302, and to the Office of Management and Budget, Paperwork Reduction Project (0704-0188), Washington, DC 20503

1. AGENCY USE ONLY (Leave blank) 2. REPORT DATE 1994 3. REPORT TYPE AND DATES COVERED Reprint

4. TITLE AND SUBTITLE (see title on reprint) 5. FUNDING NUMBERS PE: NWED QAXM WU: 00145

AD-A283 002

6. AUTHOR(S) Swenberg et al.



7. PERFORMING ORGANIZATION NAME(S) AND ADDRESS(ES) Armed Forces Radiobiology Research Institute 8901 Wisconsin Ave. Bethesda, MD 20889-5603 8. PERFORMING ORGANIZATION REPORT NUMBER SR94-13

9. SPONSORING/MONITORING AGENCY NAME(S) AND ADDRESS(ES) Uniformed Services University of the Health Sciences 4301 Jones Bridge Road Bethesda, MD 20814-4799 10. SPONSORING/MONITORING AGENCY REPORT NUMBER 94-24132

11. SUPPLEMENTARY NOTES DTIC ELECTE AUG 01 1994 S G D 2090

12a. DISTRIBUTION/AVAILABILITY STATEMENT Approved for public release; distribution unlimited. 12b. DISTRIBUTION CODE

13. ABSTRACT (Maximum 200 words) Accession For NTIS CRA&I [checked] DTIC TAB [checked] Unannounced [ ] Justification By Distribution/ Availability Codes Dist Avail and/or Special A-1 20

14. SUBJECT TERMS 15. NUMBER OF PAGES 21 16. PRICE CODE 064

17. SECURITY CLASSIFICATION OF REPORT UNCLASSIFIED 18. SECURITY CLASSIFICATION OF THIS PAGE UNCLASSIFIED 19. SECURITY CLASSIFICATION OF ABSTRACT 20. LIMITATION OF ABSTRACT

**SECURITY CLASSIFICATION OF THIS PAGE**

**CLASSIFIED BY:**

**DECLASSIFY ON:**

**SECURITY CLASSIFICATION OF THIS PAGE**



Pergamon

ARMED FORCES RADIOBIOLOGY  
RESEARCH INSTITUTE  
SCIENTIFIC REPORT  
SR84-13

Adv. Space Res. Vol. 14, No. 10, pp. (10)181-(10)201, 1994

1994 COSPAR  
Printed in Great Britain. All rights reserved.  
0273-1177/94 \$7.00 + 0.00

## ENERGY AND CHARGE LOCALIZATION IN IRRADIATED DNA

C. E. Swenberg,\* L. S. Myers, Jr\* and J. H. Miller\*\*

\* *Armed Forces Radiobiology Research Institute, 8901 Wisconsin Avenue, Bethesda,  
MD 20889-5603, U.S.A.*

\*\* *Pacific Northwest Laboratory, PO Box 999, Richland, WA 99352, U.S.A.*

### ABSTRACT

The relation between the site of energy deposition and the site of its biological action is an important question in radiobiology. Even at 77°K, evidence is clear that these two sites must be separated since energy deposition is random but specific products are formed. Several processes that may contribute to this separation are: 1) hole migration and stabilization through deprotonation to give neutral oxidation product radicals; 2) electron trapping and transfer to form specific radical anions, possibly followed by protonation to give neutral reduction product radicals; and 3) recombination of spatially separated charges or radicals. These microscopic processes will be reviewed critically in an analysis using electron paramagnetic resonance spectroscopy (EPR) evidence for and against long-range transfer of energy and/or charge in frozen, hydrated DNA.

### INTRODUCTION

A strongly held tenet of radiobiology is that damage of DNA mediates many of the cellular effects of ionizing radiation. Whether the damage results from attack on DNA by ·OH (hydroxyl free radical) or other radicals formed at a distance from a DNA molecule (indirect effect) or from energy deposited directly in a DNA molecule by radiation (direct effect) has been the subject of debate for many years /1/. Growing evidence indicates that the direct effect, defined to include deposition of energy in DNA and water molecules closely associated with DNA (the hydration layer or layers) plays a critically important role in cellular responses to radiation /2,3/. It follows that investigations of the localization of energy and charge in irradiated DNA are urgently needed.

Experimental studies have shown convincingly that the radiation chemistry of DNA is critically dependent on experimental conditions. The type of salt and its concentration /4/, and the state of DNA hydration /5,6,7/ are among the variables that effect

DTIC QUALITY INSPECTED 8

DNA chemistry. EPR spectroscopy has provided a most valuable experimental tool to develop insight into the fundamental processes involved in DNA damage reactions. EPR spectra ranging from a 0.9mT "singlet" spectrum to a 14mT octet spectrum were reported for irradiated DNA as early as 1972 /8/. Sorting out the factors contributing to spectral variation has taken the efforts of many outstanding investigators. A major contribution in elucidating DNA radiation chemistry at low temperature was the preparation by Rupprecht /9/ of oriented DNA fibers by the wet spinning technique. Samples prepared in different ionic environments have made it possible to compare the radiolysis products of DNA obtained with different types of radiation and with different orientations of the DNA fiber axis relative to the radiation beam direction. Results have been surprising. We note here that exposure of such samples to gamma radiation at 77°K and measured at 77°K resulted in EPR spectra interpreted in terms of G radical cations\* and T and/or C radical anions /10,11/. Exposure of samples

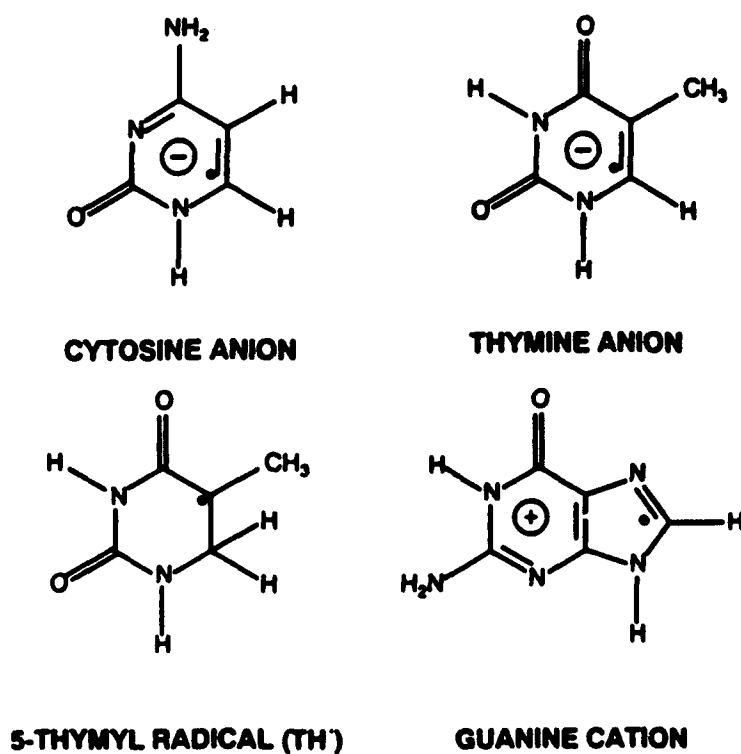


Fig. 1. Free radicals identified by EPR spectroscopy at 77°K in DNA irradiated at 77°K.

under similar conditions to neutrons resulted in similar spectra if the neutron beam was perpendicular to the DNA helix axis; however, if the beam was parallel to this axis, the EPR spectra indicated the presence of the neutral radiation product, the dihydrothymidin-5-yl (TH<sup>•</sup>) radical /12/. For proton irradiation, however, the TH<sup>•</sup>

---

\*The following symbols are used for the DNA bases: G=guanine; A=adenine; C=cytosine; T=thymine

spectrum was observed with both parallel and perpendicular beam orientations /13/. Figure 1 summarizes the free radicals identified in irradiated DNA at low temperatures.

Attempts have been made to explain these results in terms of a variety of microscopic long-range transfer mechanisms, such as triplet exciton migration /12,14/, polaron transport /14/ and solitons /14/. We discuss these mechanisms critically in view of recent research advances. We first consider whether the occurrence of different radicals produced by different kinds of ionizing radiation are artifacts or properties of the systems. We then address whether the microscopic energy deposition pattern is sufficient to explain the results or whether long-range migration of energy and/or charge is required and how this migration might best be described.

Specifically, we question whether neutral triplet or singlet state migration provides an explanation of the neutron results. This is followed by a short discussion as to whether solitons or other DNA collective states or polaron transport are involved in the neutron and proton results. We then address whether other microscopic track phenomena are operative. Charge recombination and charge trapping in dense particle tracks are briefly discussed and their effects on total radical yields are summarized. The paper concludes with a brief discussion of the reaction(s) that might account for the appearance of TH' at low temperatures and concludes with suggestions for plausible future research.

## EXPERIMENTAL BACKGROUND SUMMARY

Samples: All experiments were performed at 77°K with either oriented Na-DNA samples prepared by Rupprecht /9/ using the wet spinning technique or in some of the neutron experiments, by Arroyo et al. /12/ using the procedure of Rupprecht. Samples for the proton irradiations were carefully prepared because of the proton's short-range in the target medium, approximately 0.5 mm for 4 MeV protons. For experiments in which the DNA fibers were oriented perpendicularly to the beam, samples were made by pressing together a sufficient number of sheets of oriented DNA to give a sample thickness greater than the proton range. For the parallel proton irradiation configuration, samples were carefully sliced from a block of oriented DNA so that the ends of samples were not bent over so as to introduce spurious perpendicular components into the EPR data. Although the samples used for the proton experiments were approximately two years old, they were preserved under controlled conditions. X-ray diffraction studies on several specimens (personal communication, A. Rupprecht) demonstrated some distortions due to the pressure required to make the DNA film layers stick together in the original preparation and in the original splicing of the samples, but nothing significant to preclude failure to observe possible orientation effects. The DNA conformation /15/ as determined from independent samples is a mixture of the A-DNA form, where base planes are at 70° angles to the helix axis, and the B-DNA form (57%), where base planes form right angles to the DNA helix axis. All samples were equilibrated with water vapor at 75% relative humidity; this gives a moisture content sufficient to almost fill the primary DNA hydration shell /16/. Figure 2 gives a plot of the number of water

molecules per nucleotide as a function of the relative humidity in the hydration chamber *17*.

Figure 2 emphasizes that even at 0% relative humidity, there are 2.5 H<sub>2</sub>O molecules attached to the sodium phosphate groups per nucleotide. These water molecules are not removable via vacuum desiccation of DNA samples *17*. For our purpose we note that the tightly bound H<sub>2</sub>O molecules (the first 12-15 water molecules) are impermeable to cations *18*. Another characteristic of this inner hydration shell is that it does not form an ice-like structure. The addition of approximately nine more H<sub>2</sub>O molecules per nucleotide completes the filling of DNA primary hydration layer. It is in this latter layer of water molecules where charge transfer could possibly occur. Thus for a relative humidity of 75% the outer hydration layer is nearly filled, and furthermore contains sufficient water molecules to support charge transport along the DNA backbone.

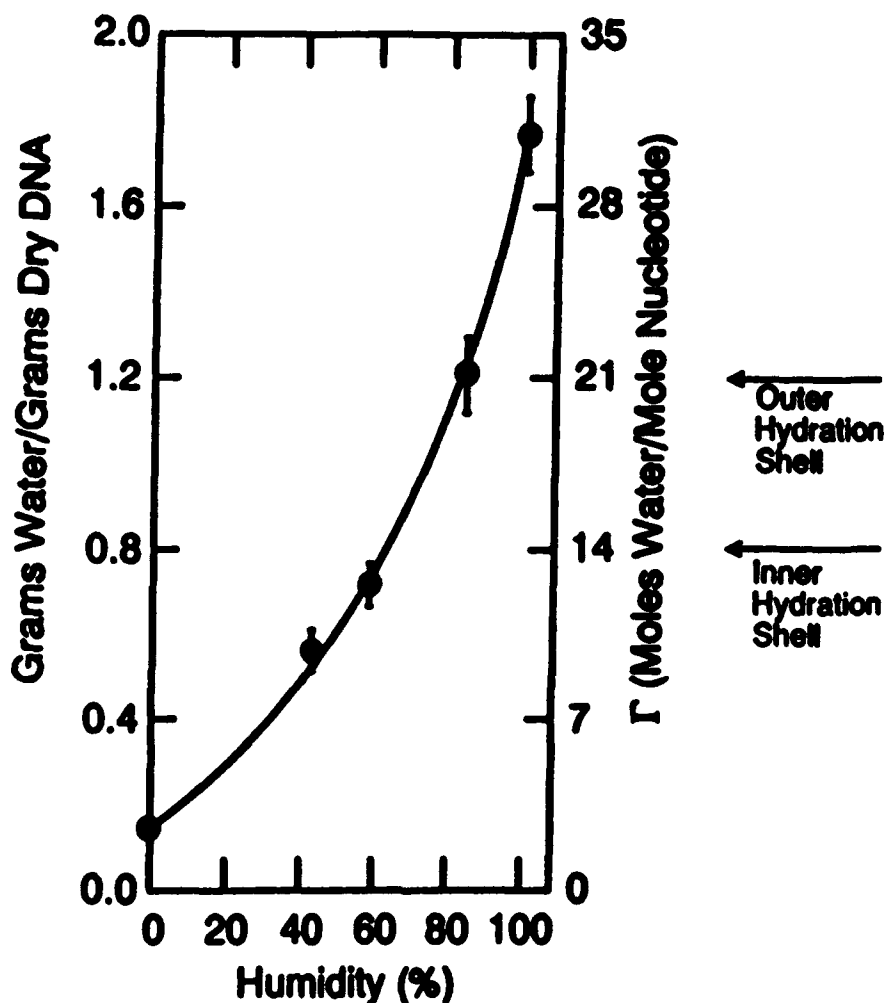


Fig. 2. Hydration of double stranded salmon sperm DNA as a function of relative humidity *17*.

**Radiation Sources:** The gamma radiation /10,11/ was from a  $^{60}\text{Co}$  source. The neutron source was a small TRIGA research reactor. Bismuth shielding was utilized to reduce the gamma component to less than 3% of the total dose. This procedure (unfortunately) introduces a broad neutron spectrum (neutron with energies of  $10^4\text{eV}$  to more than  $10^7\text{eV}$ ) with a broad peak near 1 MeV. Doses were measured by an indium foil technique. The principle neutron reaction for this energy range in tissue-like (water-like) media is elastic scattering of protons. The divergence of the neutron beam induces a diverging recoil proton beam suggesting that any orientation effects observed with neutrons might well be enhanced if a well collimated proton beam were employed. Such beams were obtained from a 2 MV tandem accelerator that provided monoenergetic protons with energy up to 4 MeV. As protons have short track ranges at these energies, only the front surfaces of the DNA samples were irradiated. Table 1 summarizes the parameters for the three experiments.

**Table 1** Irradiation Parameters

Investigator	Radiation	Dose (kGy)	Dose-Rate (kGy/hr)
Graslund et al. /4,5/	Gamma	5	9
Arroyo et al. /7/	Neutron	15	25
Miller et al. /8/	Proton	50	150

**EPR Analysis:** X-band EPR spectra at 100 kHz and 1 to 2 gauss modulation amplitude were obtained with microwave powers of  $< 3\mu\text{W}$  (gamma experiments),  $20\mu\text{W}$  for spectra perpendicular to the incident neutron beam,  $200\mu\text{W}$  for the parallel radiation configuration and  $12.5\text{mW}$  for the proton experiments. Lower power was used in the gamma experiments to avoid saturation of the ion radical signals.

## RESULTS

Irradiation with gamma rays resulted in the spectra shown in Figure 3 /10/. These spectra were interpreted as indicating the presence of the guanine radical cation and the thymine or cytosine radical anion. Recent studies of Bernhard /19,20,21/ indicate that the anion probably is a cytosine and that it may well be protonated /21/. Steenken /22/ has stressed the importance of protonation in influencing electron

attachment. For example, within a base pair, proton transfer will stabilize one electron reduction of cytosine. Bernhard /19/ has shown that the probability of electron attachment follows the relation  $T > C \gg A > G$ , which is in agreement with calculated electron affinities of the bases /23,24/. The stacking in duplex DNA in aqueous media, however, permits electron transfer between the bases, and proton transfer from a hydrogen bonded partner may occur. Thus the tendency of the hydrogen bonded partner to deprotonate becomes an important factor. The observation that A is a poorer proton donor than G means that  $C^{\cdot-}$  is stabilized by base pairing more than  $T^{\cdot-}$ . Bernhard /19/ has shown that the following relative concentration relationships are expected in double stranded DNA:  $[C^{\cdot-} H^{\cdot}] \gg [A^{\cdot} H^{\cdot}] = [T^{\cdot}] \gg [G^{\cdot}]$ . Note that thymine is the only base that should strongly form an electron adduct but is unlikely to protonate reversibly in this environment. On heating the sample and then recooling to 77°K the EPR spectrum shows the formation of neutral  $TH^{\cdot}$  radicals /10,11/, and the disappearance of the ionic radicals and a reduction in the number of total spins. This is critically important in the explanation for the appearance of  $TH^{\cdot}$  radicals.

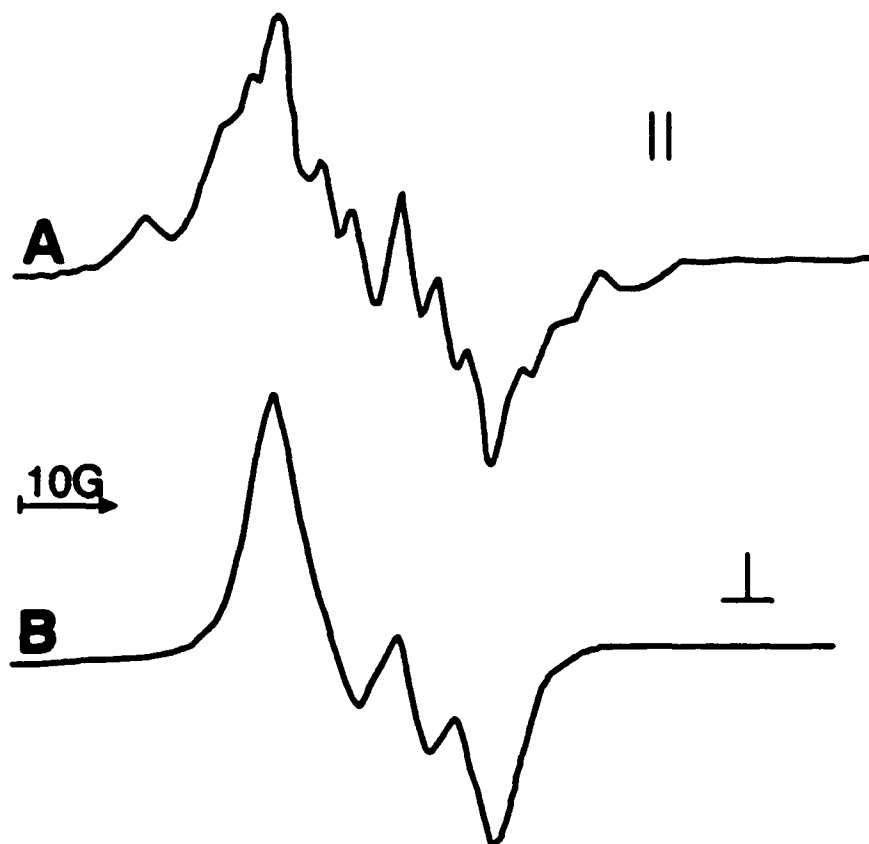


Fig. 3. EPR spectra of calf-thymus Na DNA irradiated with gamma rays /10/.

In contrast to the gamma-induced spectra, proton irradiation gave the spectra shown in Figure 4 /13/, indicative of the presence of neutral  $TH^{\cdot}$  radicals. Spectra are similar both for parallel and perpendicular irradiation configuration. For neutron irradiation the EPR spectra obtained at 77°K are shown on Figure 5.

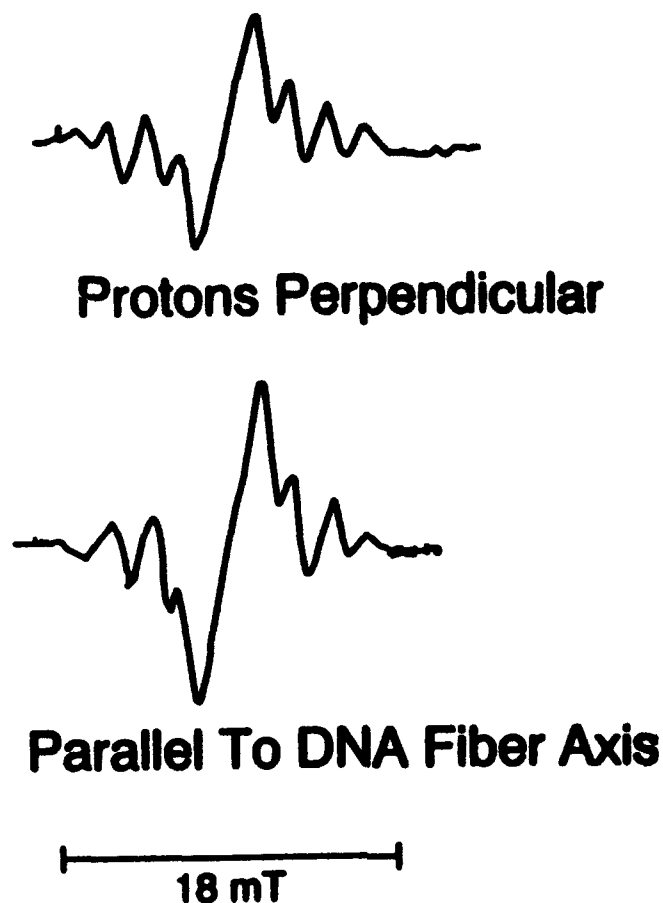


Fig. 4. EPR spectra at 77°K with 4 MeV protons /13/.

When the neutron beam was directed parallel to the DNA fiber axis, the neutral radical  $\text{TH}^\cdot$  was formed; however, when the incident neutron flux was perpendicular to the fiber axis, the spectra showed the presence of radical anions. The EPR data raise the following questions: (1) by what mechanism(s) does proton radiation give the neutral protonated reduction product ( $\text{TH}^\cdot$ ) whereas gamma radiation at 77°K gives only ionic products? and (2) by what mechanism(s) does neutron irradiation give spin products dependent on the direction of the neutron beam?

Are the results with protons and neutrons due to some problem with the experimental procedures? We have conducted an extensive review of the procedures used for the neutron and proton experiments. In the neutron experiments, two samples were mounted side by side within a liquid nitrogen cooled irradiation chamber so that the fiber orientation of one sample was perpendicular to the neutron beam and the orientation of the second sample was parallel to the incident beam. The samples, irradiated simultaneously, were treated identically so far as is known. Furthermore the experimenters successfully observed the ion radical signals after gamma irradiations, and samples prepared by Rupprecht and by Arroyo /12/ gave the same results. While, of course we can not completely eliminate the possibility that errors were made, we have considerable confidence in the results.

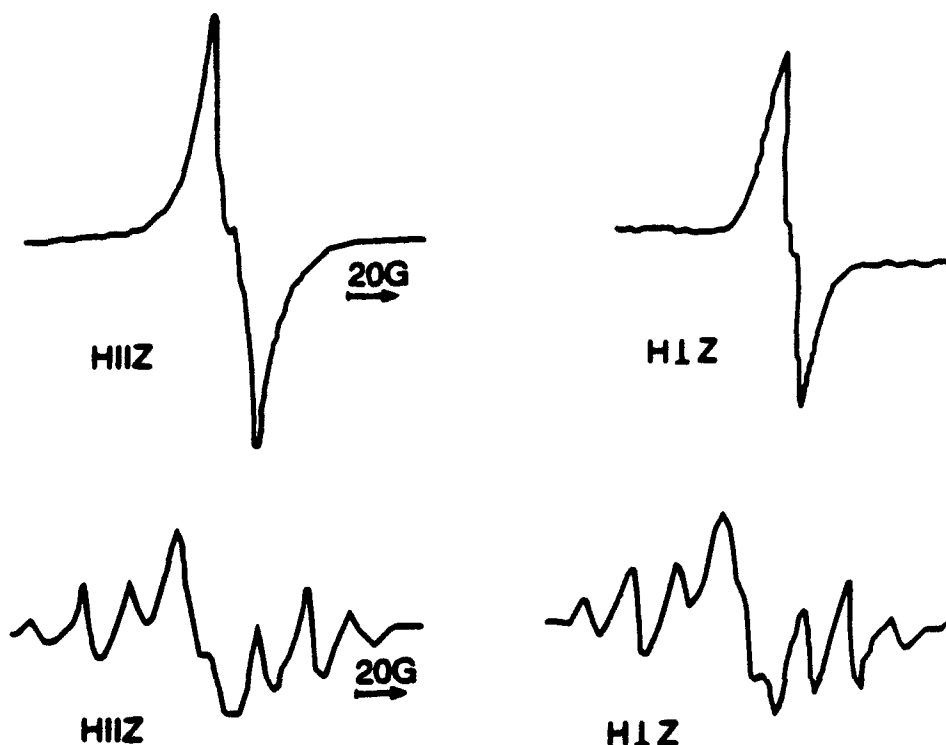


Fig. 5. EPR spectra from calf-thymus Na DNA irradiated with TRIGA-reactor neutrons /12/.

For the proton study, individual samples were irradiated in a liquid nitrogen cooled chamber and transferred to the EPR cavity. During the transfer the samples were exposed to a temperature  $> 77^{\circ}\text{K}$  for less than one second. Comparing this time with the times at various temperatures required for the appearance of  $\text{TH}^{\cdot}$  /11/, we feel confident that this step does not account for the results. Furthermore, the samples were examined by Rupprecht, and by his criteria, which included determination of X-ray diffraction patterns, they were satisfactory for the experiment. Thus we conclude that the results are not a consequence of any obvious or apparent experimental problem.

In the proton experiments, are the results due to macroscopic heat build-up during the irradiation accompanied by inefficient heat transfer from sample to coolant? Elementary calculations show that if all the energy deposited in the sample were retained and converted to heat, the temperature increase would be of the order of  $10^{\circ}\text{K}$ . Using reasonable estimates of the cooling, and considering the dose rate, etc., we estimate a temperature difference of about  $.002^{\circ}\text{K}$  between the thermal reservoir at  $77^{\circ}$  and the irradiated part of the sample. Such a small temperature difference, even if underestimated by a factor of  $10^3$  would not be nearly enough to cause the formation of  $\text{TH}^{\cdot}$  by the reaction path observed by Gräslund and coworkers /10,11/.

Does heat generated within the proton tracks in both the proton and neutron experiments explain the appearance of the protonated thymine? Several investigators /25,26,27/ have suggested that fast heavy ions with large stopping power result in

transient localized heated regions around the ion tracks. To estimate this effect we follow the treatment given by Mozumder /28/ who adopted a Gaussian statistical approximation. Solving the standard macroscopic heat equation for low LET radiation one finds the distribution of the excess temperature, where the spur is approximated by a sphere with size parameter  $r_0$ , to be:

$$\Delta T^{(1)}(r,t) = T_0 (1 + 4\delta t/r_0^2)^{-3/2} \exp\{-r^2/(r_0^2 + 4\delta t)\}$$

Here  $T_0$  is the maximum excess temperature at the spur's center,  $r$  is the distance from the spur center, and  $\delta$  is the thermal diffusivity and equals  $X/\rho C_v$ , the heat conductivity ( $X$ ) divided by the product of the medium density ( $\rho$ ) and specific heat ( $C_v$ ) at constant volume.  $T_0$  is determined by the relationship:

$$E = \int_0^{\infty} \rho C_v T_0 4\pi r^2 \exp(-r^2/r_0^2) dr$$

where  $E$  denotes the average energy deposited per charge pair in the spur,  $\approx 30\text{eV}$ . For high LET ionizing particles traversing a medium a large number of phonons are created resulting in a high density of transient temperature pulses. These heated regions overlap and thereby form a cylindrical excess thermal distribution with initial radius  $r$ , that can be approximated as:

$$\Delta T^{(3)}(r,t) = T_0 (1 + 4\delta t/r_0^2)^{-1} \exp\{-r^2/(r_0^2 + 4\delta t)\}$$

where  $r$  is the transverse distance from the track axis. If  $S$  denotes the energy loss per unit distance, then

$$S = \frac{dE}{dx} = \int_0^{\infty} \rho C_v T_0 2\pi r \exp\{-r^2/r_0^2\} dr$$

determines the initial temperature  $T_0$  at the center of the cylindrical track. Figures 6A and 6B illustrate the time dependence of local heating for several  $r$  values assuming  $\delta = 10^3 \text{cm}^2/\text{sec}$ ,  $r_0 = 20\text{\AA}$ ,  $E = 30\text{eV}$  and  $S = 5\text{eV/\AA}$ .

Variations for  $\Delta T$  are quite similar and in both cases decay to the ambient temperature in approximately  $10^{-10}$  to  $10^{-9}$  seconds. Although these calculated temperature transients are similar, the effect of the heat spike on reaction rates is strongly dependent on dimensionality. Assuming an activation energy of 8 Kcal/mole, a substrate concentration of  $10^{22}$  molecules/cm<sup>3</sup> and a collision frequency of  $10^{11} \text{s}^{-1}$

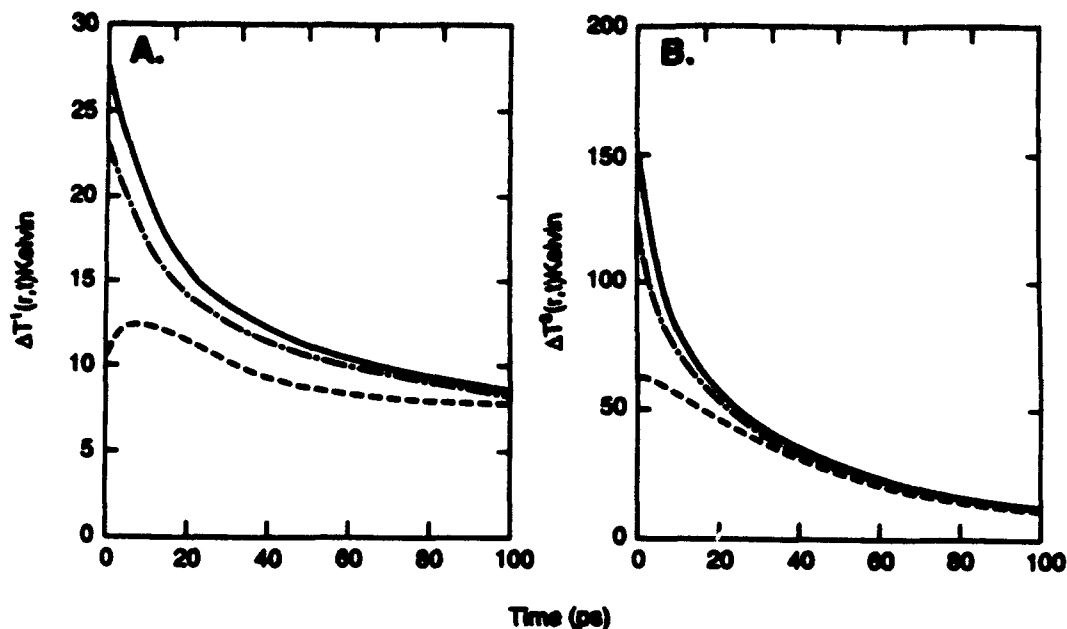


Fig. 6. Excess temperature transients (A)  $\Delta T^{(1)}(r,t)$  in a spur (low-LET radiation) and (B)  $\Delta T^{(3)}(r,t)$  in a cylindrical track (high-LET radiation) at several distances (—,  $r = 10 \text{ \AA}$ , ---,  $r = 15 \text{ \AA}$ , and - · - · -,  $r = 20 \text{ \AA}$ ) from the center of the spur or the cylindrical track axis.

$$K = 10^{11} \exp\{-8000/RT\} \text{ cm}^3 \text{ s}^{-1} / \text{molecule}$$

gives a low LET reaction time of  $\approx 0.5 \mu\text{sec}$  (assuming  $T_0 = 400^\circ\text{K}$ ). For high LET irradiation with  $S = 500 \text{ eV/\AA}$  corresponding to a  $T_0$  of  $10^4 \text{ }^\circ\text{K}$  ( $RT = 0.83 \text{ eV}$ ) the reaction time is estimated to be  $1.5 \times 10^{-11} \text{ sec}$ , a time comparable to the duration of the thermal pulse. This simple calculation demonstrates that, at least for low LET radiation, the induced transient increase in the local temperature does not effect chemical processes. This, however, need not be valid for very high LET radiation since the temperature pulse duration can be comparable to chemical reaction times.

Similar calculations for 4 MeV proton tracks yields an initial temperature of about  $100^\circ\text{K}$ , which is probably not sufficient to stimulate the formation of  $\text{TH}^\cdot$ . However, errors in the estimates could well bring the temperature into the necessary range of about  $200^\circ\text{K}$ . Thus intra-track heating by proton radiation during and shortly thereafter can not be excluded as a possible mechanism involved in the formation of  $\text{TH}^\cdot$ .

Several microscopic processes have been suggested to explain the observed anisotropy in the neutron experiments. We discuss briefly whether any of the quasi-particles, excitons, solitons or polarons or other track phenomenon can account for the anisotropic neutron EPR spectra.

Does the migration of triplet and/or singlet excitons provide an explanation of the neutron EPR spectra? In the original paper by Arroyo et al /12/ it was suggested that the migration of triplet states might provide an explanation of the neutron EPR data. We now believe this transport mode cannot provide the large asymmetry in the transport of energy in DNA (see the discussion on microscopic intra-track spike model) needed to account for the neutron data. Both singlet and triplet exciton migration (within oriented DNA) is probably limited to at most 10 base pairs due to their short life time and extensive trapping expected to exist in highly disordered systems. Although excess hole and electron band widths along the DNA sugar-phosphate backbone are estimated to  $\approx 400 \text{ cm}^{-1}$  and  $1200 \text{ cm}^{-1}$ , respectively /29/, the neutral excited state is considerably narrower, about  $10$  to  $70 \text{ cm}^{-1}$  /30/. These theoretical values, although admittedly crude, support the contention that mobile neutral excited states have very short transfer distances. Numerous experiments support this viewpoint. As an example we note that exciplex formation in DNA is a rapid process /31/ estimated to be the order of  $10^{12} \text{ sec}^{-1}$ ; thus excited singlet transfer needs to occur in less than  $10^{-12} \text{ sec}$ . Denoting the mean transfer distance by  $d_s$ , we have

$$d_s^2 = 2Fa^2t_T$$

if only nearest neighbor transfers are considered with a Förster rate  $F \approx 10^{13} \text{ sec}^{-1}$ . Here  $a$  is the neighboring base pair stacking distance (0.34nm in B-DNA) and  $t_T$  is the trapping time. Assuming an exciplex formation time of  $10^{-12} \text{ sec}$  gives a transfer distance  $d_s$  of 1.5 nm or approximately 4 to 5 base pairs. Triplet state transfer has been investigated by Eisinger and Lamola(32) and by Gueron and Shulman (33) to note but a few. Probably the most definitive experimental evidence for triplet migration in DNA has been provided by measuring the quenching of DNA phosphorescence by metal ions. Analysis of the data by Isenberg and coworkers (34) on  $\text{Ni}^{2+}$ ,  $\text{Co}^{2+}$  and  $\text{Mn}^{2+}$  quenching gives triplet transfer distances comparable to that of the singlet state, (0.8 to 1.5 nm). We therefore can safely conclude that neutral state migration range is short in DNA and does not constitute an effective mechanism.

Does a microscopic temperature spike model using theoretical track codes account for the anisotropy in neutron EPR data? The most obvious difference in the pattern of energy absorption in the two irradiation geometries is that charged particles traversing the sample nearly parallel to the helical DNA axis have a greater probability for multiple energy transfers to the same DNA molecule than do particles incident on the sample perpendicular to the fiber orientation. This difference in the spatial pattern of energy absorption should have no effect on the production of free radicals if energy and/or charge move between different DNA fibers as freely as they

are transported along a single DNA chain. The macroscopic model developed by Miller *et al.* /35/ (the quasi particle being transported is not identified) assumes that an orientation dependence of radical yields is indicative of intramolecular energy and/or charge transfer in DNA. The asymmetric 3-dimensional heat equation is solved in the limit where only the shortest transverse relaxation time ( $\tau_t = b^2/5.8D_t$ , where  $b$  is the DNA radius and  $D_t$  is the transverse diffusion coefficient) is included. Miller *et al.* showed that in this approximation the local temperature at energy deposition site  $x_k$  (determined by Monte Carlo track simulation) and at time  $t$  is given by

$$T(x,t) = T_s + \exp(-t/\tau_t) \sum_k T_k(x,t/\tau_t)$$

and

$$T_k(x,t) = T_{ko} (1 + t/\tau_l)^{-1/2} \exp\left\{\frac{-(x-x_k)^2}{2\Delta^2(1 + t/\tau_l)}\right\}$$

where  $T_s$  is the ambient sample temperature,  $\tau_l = \Delta^2/2D_l$  is the longitudinal thermal relaxation time,  $D_l$  is the longitudinal diffusion coefficient,  $\Delta$  is the half-width of the superexcited state (taken to be 3.4Å, the nearest neighbor base-pair distance) and

$$T_{ko} = \epsilon_k/b^2\Delta\rho C(2\pi^3)^{1/2}$$

where  $C$  and  $\rho$  are the specific heat and sample density and  $\epsilon_k$  is the absorbed energy at site  $x_k$ .

An essential difference between the Henriksen *et al.* /26,27/ application of "heat waves" to calculate conversion of the primary radicals in proteins and the thermal spike model of Miller and coworkers /35/ is that of reformulating the thermal spike model in terms of track structure rather than simply stopping power. In view of recent findings by Bernhard /19,20,21/, electrons liberated in the decay of superexcited states by autoionization (see Figure 7) eventually form  $C^{\cdot}$ .

Energy from other deposition events in the same DNA chain are treated as temperature spikes that spread throughout the sample asymmetrically. Thermal diffusion along DNA chains is assumed to be 1000 fold higher than the transverse thermal diffusion. Although at present we are unaware of any experimental evidence to support this large value, it should be noted that anisotropy in electrical conductivity greater than 100 has been reported for organic systems such as polydiacetylene /36/. The longitudinal diffusion coefficient was taken to be comparable to  $H_2O$  ( $10^{-3}$

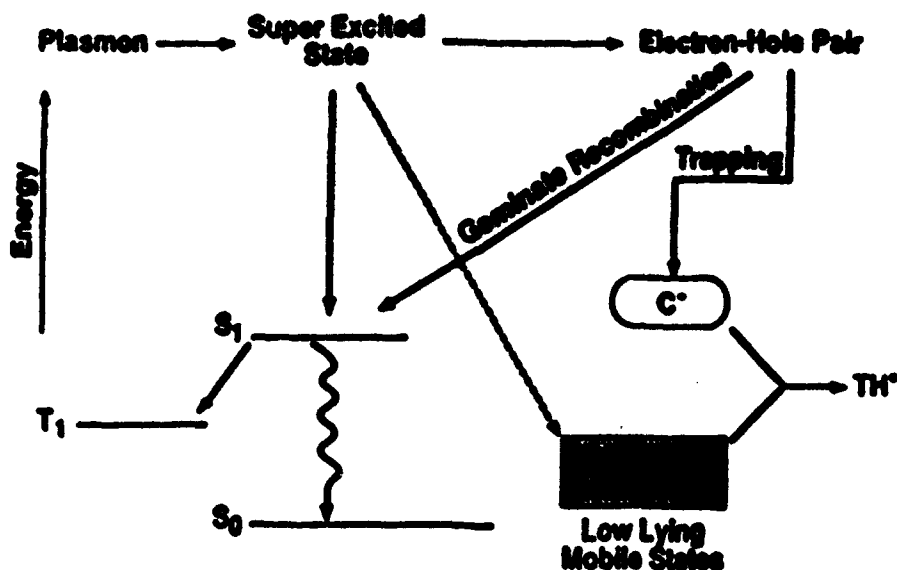


Fig. 7. Possible decay modes of energy absorbed from ionizing radiation in hydrated DNA samples.

$\text{cm}^2 \text{sec}^{-1}$ ) and protonation of the thymine radical was approximated by quasi first-order kinetics with an activation energy between 0.2 and 0.6 eV. The mechanism for conversion of primary radical anions to  $\text{TH}\cdot$ , which probably involves electron transfer from C to T followed by irreversible protonation at C6, is assumed to be the same as that which operates in thermal annealing experiments /11/. Although the model does predict greater conversion of primary radical anions to  $\text{TH}\cdot$  for a proton flux oriented parallel to the DNA fibers, it cannot account for the 3 fold greater total radical yields observed in the parallel neutron irradiation configuration without additional considerations of electron trapping and ion recombination. Furthermore, the model predicts that both primary radical anions and  $\text{TH}\cdot$  should be seen in the parallel case, which does not agree with the observations reported by Arroyo et al. /12/ where radical anion species were detected in the only in the perpendicular case.

Are solitons involved in energy transfer in DNA? Solitons have been proposed as a mechanism of long-range energy transfer in DNA /14,37,38/. These collective states have been invoked to explain the hydrogen-deuterium exchange reaction observed in double-stranded polynucleotides /39,40/; however, problems with this explanation have been noted by Benight et al. /41/. There is currently no generally accepted theory of solitary waves in DNA. As a first approximation, one might visualize a DNA solitary wave as a configuration formed by partial underwinding of the helix over several base pairs with some disruption of interstrand hydrogen bonds. Yomosa /42/ developed a simple DNA soliton model that allows one to estimate their lowest energy  $E_0$ , size  $L_0$ , and velocity  $v_0$  by fitting model Hamiltonian calculations to the temperature dependence of the equilibrium constant for hydrogen-deuterium exchange /40/. Although details of the Yomosa model of open states are likely to be incorrect (e.g. the assumption of complete base-pair rotation about the phosphate-sugar backbone and the neglect of DNA backbone bending energy), it does provide reasonable estimates of the above parameters. Under the assumption that base stacking is preserved in soliton excitation and with a Hamiltonian which includes interstrand hydrogen bonding, intrastrand stacking, and torsional energy, Yomosa /42/

calculated  $E_0 = 0.35$  eV, which is sufficient to overcome the activation barrier to irreversible protonation of pyrimidine radical anions at C6,  $L_0 = 10$  base pairs, which demonstrates the non-local character of this excitation mode, and  $v_0 = 8.3 \times 10^3$  cm/sec, which is less than the velocity of sound in DNA as it should be.

The soliton migration distance  $d$  can be estimated by noting that in the radiation-induced thermal spike model of Miller *et al.* /35/, the heat wave has a lifetime of approximately 1 ns, a value considerably shorter than the measured open-state lifetime of  $10^{-7}$  s /43/; thus  $d = 83$  nm. Hence, intramolecular energy transfer by solitons is a credible mechanism for the necessary long-range energy transfer inferred from Monte Carlo calculations /35/ to explain the neutron data. Unfortunately, a soliton model without charge recombination and trapping cannot account for the observed neutron-induced radical yields. This limitation might be removed by inclusion of the effects of soliton pinning; however, a theory of this process in DNA is not currently available.

Is polaron transport involved in the neutron or proton results? It is possible that long-range migration (LRM), either by electrons or protons could account for the neutron data. Charge transfer in organic systems is well documented /30/. Transport through stacked DNA bases has been shown by van Lith and coworkers /44/ to be the order of 9 nm, which is not long enough to explain the presence of  $\text{TH}\cdot$  radicals at 77°K. Furthermore, these investigations demonstrated that transport through the phosphate-sugar backbone is also not sufficient. Experimental data do, however, support the possibility of LRM within the structured water layers of DNA hydration. Using transient microwave techniques, van Lith *et al.* /44/ observed a mobility  $\mu$  of  $2.5 \times 10^{-3} \text{ m}^2 \text{ V}^{-1} \text{ sec}^{-1}$ , which they associate with transfer of "dry" electrons in the water layer, provided the water concentration was above the critical weight fraction  $F_0 = 0.44$ . For comparison, mobilities of  $2 \times 10^{-6} \text{ m}^2 \text{ V}^{-1} \text{ sec}^{-1}$  and  $1 \times 10^{-4} \text{ m}^2 \text{ V}^{-1} \text{ sec}^{-1}$  have been reported for horizontally stacked phthalocyanine columns /45/ and polyethylene /46/, respectively. Above the critical water content, the conductivity is linear in  $F$ . If the carrier lifetime (determined primarily by trapping at defects) is an order of magnitude longer than the unsolvated electron in pure ice, then the mean transfer distance at -78° C is about 100 nm. More recent estimates by Warman *et al.* /45/ give a maximum transfer distance of only 115 base pairs or about 40 nm.

Although electron transfer is sufficient to explain LRM in DNA, proton transport is another possibility. Kunst and Warman /47/ attributed the longer-lived conductivity transient for ice (after electrons are trapped) to mobile protons. If this is the case, then narrow-band polaron transport /48/ is the appropriate theoretical formalism to describe the dependence of mobility on temperature. In this theory

$$\mu = (ea^2/kT) \pi^{1/2} v_0 F(T)^{1/2} \exp(-F(T))$$

with

$$F(T) = 2w_p/hv_0 \operatorname{csch}(hv_0/2kT)$$

where  $w_p$  is the polaron binding energy,  $a$  is the interatomic distance, and  $v_0$  is the vibrational frequency of the phonon that interacts most strongly with the carrier. Using these equations, we estimate that the proton mobility in hydration layers of DNA is between  $0.1$  and  $1 \text{ cm}^2 \text{ V}^{-1} \text{ sec}^{-1}$  at  $77^\circ\text{K}$ . To achieve a migration distance of  $100\text{nm}$ , protons with mobilities in this range would require lifetimes of  $4$  to  $40 \text{ ns}$ , which are consistent with existing results on the trapping of electrons and protons in ice /47/. Hence, mechanisms of charge transport exist with sufficient range to account for the orientation effect on radical types reported for neutron irradiation but, as was the case for the thermal spike model, trapping and recombination must be included in any model of radical yields.

What is the role of carrier trapping and recombination in explaining existing EPR data? As noted above, considerations of trapping and recombination in addition to LRM of any quasi-particle are needed to explain the factor of 3 difference between total radical yields observed in parallel and perpendicular neutron irradiation /12/. Miller and Swenberg /38/ have suggested ways to model this effect as well as the absence of  $\text{TH}\cdot$  radicals in the perpendicular configuration. The observations of van Lith et al. /44/ of electron LRM in hydrated DNA following nanosecond pulses of  $3 \text{ MeV}$  electrons suggest that autoionization of superexcited states (as illustrated in Fig. 7) produces quasi-free electrons in the hydration layers of DNA where they undergo LRM before relaxation into another trap. Films of oriented DNA may be similar in some respects to the quasi-one-dimensional semiconductors illustrated schematically in Figure 8, below. In the perpendicular irradiation configuration, yields of primary radical anions and cations are mainly determined by the competition between geminate recombination and electron trapping at preexisting defects (denoted by squares in Fig. 8). In the parallel case, the high mobility path of electrons (for polydiacetylene mobility parallel to the fiber direction can be 100 times greater than mobility perpendicular to the fibers /36/) contains trapped positive ions that will reduce the radical yield by nongeminate recombination of the ionic precursors. Solution of the coupled differential equations that describe radical production and decay in this model will be given in a future publication. Here we note only that, in contrast to the soliton model depicted in Figure 7 where collective vibrational excitations are the mobile low-lying states, ejected electrons are the quasi-particle with asymmetric mobility in the model depicted in Figure 8. Vibrational excitations that accompany both the production and decay of ion pairs are assumed to be localized.

Our analysis indicates that no energy or charge transport model can fully account for anisotropy (in the neutron experiments) observed in the EPR data if the effects of carrier trapping and recombination are neglected. Geminate recombination, applicable in the low density limit where an isolated pair of oppositely charged geminate particles can be considered as an isolated system, was developed in the late 1930's by Onsager /49,50/ and was designed as the steady state solution of the

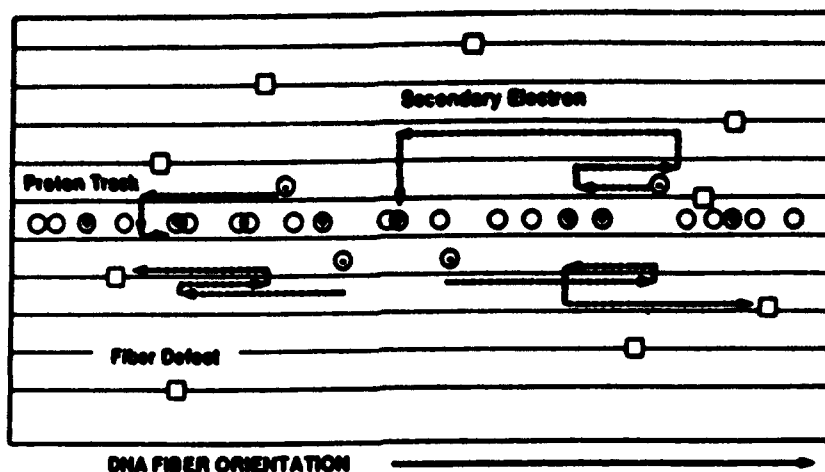


Fig. 8. Schematic diagram of electron trapping and recombination in a quasi one dimensional semiconductor. Squares and circles denote preexisting and radiation-induced traps, respectively. Broken lines represent electron trajectories. (Redrawn from /36/).

charge pair moving in a condensed phase continuum in the presence of an external electric field. This theory has been widely and successfully applied to photogeneration of carriers in organic materials (see Pope and Swenberg /30,51/ for a review). Within the past decade the theory has been extended by Hong and Noolandi /51/ to include transient effects with the refinement of replacing the original Onsager assumption of a point sink at the origin by a recombination sphere of finite radius and recombination velocity. In addition, the seminal theory of Scher and Rackovsky /52/ in which the effects of the lattice and the microscopic molecular process are considered has demonstrated the important role of competing processes, such as the decay rate of the electronically excited precursors to the ion-pair state that dissociates. This improved theory shows how the two parameters of Onsager's theory, the electron thermalization distance and the initial quantum yield of geminate pair generation can be evaluated if an assumption is made regarding the initial distribution of geminate pair distances. Recently, within the context of Onsager's continuum theory, Mozumder /54/ has illustrated by extensive numerical calculations how the fractal geometry of the lattice can influence the geminate escape probability, mean recombination time, and the reaction rate. All these theoretical treatments are applicable only in the low ionization density limit; in the cases where high LET particles are involved the free electrons, ions, and radicals in the track are so high in density that non-geminate processes are dominant (see Schott /55/). When ionization is dense, no similar results as found for geminate processes are known. This is due to two complicating factors; the repulsion between electrons and the inherent problem of tracking the amount of cation charge remaining as electron and cation are neutralized. Both of the effects have been treated in a mean field approximation although one can easily convince oneself that neither a mean field approximation nor

a perturbation approach can be successfully employed. Sano and Baird /56/ have considered the model system of two electrons in the field of a divalent cation ( a model analog of the helium atom in atomic theory). Even here the results are mathematically formidable and require numerous numerical calculations. It seems that the only viable approach is to employ a variational approach, and this obviously requires good theoretical insight on the form for the multidimensional distribution functions.

## CONCLUSIONS

Several mechanism of energy or charge transport in hydrated DNA have been proposed that have sufficient range to couple energy deposition events in DNA chains in ways that may account for the orientation dependence of radical yields in oriented DNA exposed to neutrons /12/. The details of these mechanisms will be dependent on the identity of the primary radiation-induced species; however, the concepts of relating orientation effects to energy or charge transport is independent of whether thymine or cytosine is the predominant type of electron gain center. The pattern of energy deposition events in an oriented DNA chain interacting with protons depends upon the velocity of the proton (magnitude and direction) relative to the helical axis but should be the same for a primary or secondary flux. Hence, the inconsistency between experiments with neutrons /12/ and direct proton-beam irradiation /13/ is currently the main impediment to understanding the unusual results observed with neutrons. Determining the reproducibility of these experiments is clearly the most important next step; however, a detailed analysis of the spatial distribution of energy deposited in DNA chains exposed to neutrons from the TRIGA reactor would also be helpful. If the dispersion of secondary protons makes the patterns of energy deposition in DNA chains essentially independent of their orientation relative to the neutron flux, then models for the orientation effects reported by Arroyo et al. /12/ that are based on an assumed difference in this pattern are obviously inappropriate.

## REFERENCES

1. P. Alexander and J.T. Lett, Effects of ionizing radiations on biological macromolecules, *Comprehensive Biochem.* **27**, 267 (1967).
2. J.T. Lett, Cellular radiation biology in consolidation and transition, *Brit. J. Cancer (Supplement VIII)*, **55**, 145 (1987).
3. J.T. Lett, Damage to DNA and chromatin structure from ionizing radiations, and the radiation sensitivities of mammalian cells, *Prog. Nucleic Acid Res. and Mol. Biol.* **39**, 305 (1990).
4. A. Rupprecht and B. Forslind, Variation of electrolyte content in wet-spun lithium and sodium DNA, *Biochim. Biophys. Acta* **204**, 304 (1970).

5. J.T. Lett and P. Alexander, Crosslinking and degradation of deoxyribonucleic acid gels with varying water contents when irradiated with electrons, *Radiation Res.* **15**, 159 (1961).
6. J. Hüttermann, M. Röhrig and W. Köhnlein, Free radicals from irradiation of lyophilized DNA: influence of water of hydration, *Int. J. Radiat. Biol.* **61**, 299 (1992).
7. S.G. Swarts, M.D. Sevilla, D. Becker, C.J. Tokar and K.T. Wheeler, Radiation-induced DNA damage as a function of hydration I, Release of unaltered bases, *Radiat. Res.* **129**, 333 (1992).
8. L.S. Myers, Jr. Free Radical damage of nucleic acids and their components by ionizing radiation, *Federation Proc.* **32**, 1882 (1973).
9. A. Rupprecht, Preparation of oriented DNA by wet spinning, *Acta Chem Scand.* **20**, 494 (1966).
10. A. Gräslund, A. Ehrenberg, A. Rupprecht and G. Ström, Ionic base radicals in  $\gamma$ -irradiated DNA, *Biochim. Biophys. Acta* **254**, 172 (1971).
11. A. Gräslund, A. Ehrenberg, A. Rupprecht, B. Tjälldin and G. Ström, ESR kinetics of a free radical conversion in  $\gamma$ -irradiated oriented DNA, *Radiat. Res.* **61**, 488 (1975).
12. C.M. Arroyo, A.J. Carmichael, C.E. Swenberg and L.S. Myers, Jr., Neutron-induced free radicals in oriented DNA, *Int. J. Radiat. Biol.* **50**, 789 (1986).
13. J.H. Miller, D.L. Frasco, C.E. Swenberg and A. Rupprecht, Energy transfer mechanisms in DNA: Relationship to energy deposition in submicroscopic volumes, *Radiation Research: A Twentieth-Century Perspective*, edited by W.C. Dewey, M. Edington, R.J.M. Fry, E.J. Hall, and G.F. Whitmore, (San Diego: Academic Press Inc., vol.II, p.433, 1992).
14. C.E. Swenberg and J.H. Miller, Response to "Are solitons responsible for energy transfer in DNA?", *Int. J. Radiat. Biol.* **56**, 383 (1989).
15. R. Brandes, R.R. Vold, D.R. Kearns and A. Rupprecht, A  $^2\text{H}$ -NMR study of the A-DNA conformation in films of oriented Na-DNA: Evidence of a disordered B-DNA contribution, *Biopolymers* **27**, 1159 (1988).
16. S.A. Lee, S.M. Lindsay, J.W. Powell, T. Weidlich, N.J. Tao and G.D. Lewen, A Brillouin scattering study of the hydration of Li and Na-DNA films, *Biopolymers* **26**, 1637 (1987).
17. N.J. Tao, S.M. Lindsay and A. Rupprecht, Structure of DNA hydration shells studied by Raman spectroscopy, *Biopolymers* **28**, 1019 (1989).

18. M.B. Tan and J.E. Heard, On the hydration of DNA II: Base composition dependence of the net hydration of DNA, *Biopolymers* **6**, 1345 (1968).
19. W.A. Bernhard, Initial sites of one electron attachment in DNA, NATO ASI Series, Series H: Cell Biology, Vol 54, *The Early Effects of Radiation on DNA*, E.M. Fielden and P. O'Neill, eds., Springer-Verlag, Berlin, p. 141, 1991.
20. W.A. Bernhard, Free radicals formed by electron gain in oligomers of DNA, *Free Rad. Res. Comm.* **6**, 93 (1989).
21. W.A. Bernhard, Sites of electron trapping in DNA as determined by ESR of one-electron-reduced oligonucleotides, *J. Phys. Chem.* **93**, 2187 (1989).
22. S. Steenken, Purine bases, nucleosides, and nucleotides: Aqueous solution redox chemistry and transformation reactions of their radical cations,  $e^-$  and OH adducts, *Chem. Rev.* **89**, 503 (1989).
23. N. Border, M.J.S. Dewar and A.J. Harget, Ground states of conjugated molecules XIX, Tautomerism of heteroaromatic hydroxy and amino derivatives and nucleotide bases, *J. Am. Chem. Soc.* **92**, 2929 (1970).
24. N. Berthard, C. Gressner-Prettre and A. Pullman, Theoretical study of the electronic properties of the purine and pyrimidine components of nucleic acids, I. A semiempirical self-consistent field calculation, *Theor. Chim. Acta* **5**, 53 (1966).
25. A. Norman, Thermal spike effects in heavy-ion tracks, *Radiat. Res.* **7**, 33 (1967).
26. T. Henriksen, Production of free radicals in solid biological substances by heavy ions, *Radiat. Res.* **27**, 676 (1966).
27. T. Henriksen, P.K. Horan and W. Snipes, Free-radical production by heavy ions at 77K and its relation to the thermal spike theory, *Radiat. Res.* **43**, 1 (1970).
28. A. Mozumder, Charge particle tracks and their structure, *Advances in Radiation Chemistry*, edited by M. Burton and J. Magee, (New York: Wiley-Interscience, vol.1, p.1 1969).
29. S. Suhai, Energy bands and electronic delocalization in the sugar-phosphate backbone of DNA, *Biopolymers* **13**, 1739 (1974).
30. M. Pope and C.E. Swenberg, *Electronic Processes in Organic Crystals*, (New York: Oxford University Press, 1982).
31. J.B. Birks, *Photophysics of Aromatic Molecules*, (New York: Wiley-Interscience, 1970).

32. J. Eisinger and A.A. Lamola, The excited states of nucleic acids, In: *Excited States of Proteins and Nucleic Acids*, edited by R.F. Steiner and I. Weinryb, (New York: Plenum Press, p. 107, 1971).
33. M. Guéron and R.G. Shulman, Energy transfer in polynucleotides, *Ann. Rev. Biochem.* **37**, 571 (1968).
34. I. Isenberg, R. Rosenbluth and S.L. Baird, Comparative phosphorescence quenching of DNA's of different composition, *Biophys. J.* **7**, 365 (1967).
35. J.H. Miller, W.E. Wilson, C.E. Swenberg, L.S. Myers, Jr. and D.E. Charlton, Stochastic model of free radical yields in oriented DNA at 77 K, *Int. J. Radiat. Biol.* **53**, 901 (1988).
36. E.L. Frankovich, I.A. Sokolik and A.A. Lymarev, On the photogeneration of charge carriers in quasi-one-dimensional semiconductors: polydiacetylene. *Mol. Cryst. Liq. Cryst.* **175**, 41 (1989).
37. K.F. Baverstock and R.D. Cundall, Are solitons responsible for energy transfer in oriented DNA?, *Int. J. Radiat. Biol.* **55**, 151 (1989).
38. J.H. Miller and C.E. Swenberg, Radical yields in DNA exposed to ionizing radiation: Role of energy and charge transfer, *Can. J. Phys.* **68**, 962 (1990).
39. M. Nakamshi and M. Tsuboi, Two channels of hydrogen exchange in a double-helical nuclei acid, *J. Mol. Biol.* **124**, 61 (1978).
40. H. Teitelkaum and S.W. Englander, Open states in native polynucleotides I. Hydrogen-exchange study of adenine-containing double helices. Open States in native polynucleotides II. Hydrogen-exchange study of cytosine-containing double helices, *J. Mol. Biol.* **92**, 55 (1975).
41. A.S. Benight, J.M. Schurr, P.F. Flynn, B.R. Reid and D.E. Wemmer, Melting of a self-complementary DNA minicircle: Comparison of optical melting theory with exchange broadening of the nuclear magnetic resonance spectrum, *J. Mol. Biol.* **200**, 377 (1988).
42. S. Yomosa, Solitary excitations in deoxyribonucleic acid (DNA) double helices, *Phys. Rev. A* **32**, 474 (1989).
43. M. Guéron, M. Kochovan and J.L. Leory, A single mode of base-pair opening drives imino proton exchange, *Nature* **328**, 89 (1987).
44. D. van Lith, J.W. Warman, M.P. de Hass and A. Hummel, Electron migration in hydrated DNA and collagen at low temperatures, Part 1. Effect of water concentration, Part 2. Effects of additives, *J. Chem. Soc. Faraday Trans. 1* **82**, 2933 (1986).

45. J.M. Warman, M.P. de Haas and P.G. Schouten, Charge migration in hydrated DNA, *Radiation Research: A Twentieth-Century Perspective*, edited by W.C. Dewey, M. Edington, R.J.M. Fry, E.J. Hall, and G.F. Whitmore, (San Diego: Academic Press Inc., vol.II, p.93, 1992).
46. M.P. de Haas and A. Hummel, Charge migration in irradiated polyethelene, *IEEE Transactions in Electrical Insulation* **24**, 349 (1989).
47. W. Kunst and J.M. Warman, Nanosecond time-resolved conductivity studies of pulse-ionized ice, 2. Mobility and trapping of protons, *J. Phys. Chem.* **87**, 4093 (1983).
48. G.G. Roberts, N. Appleby and R.W. Mann, Temperature dependent electronic conductivity in semiconductors, *Physics Reports* **60**, 59 (1980).
49. L. Onsager, Derivation from Ohm's Law in weak electrolytes, *J. Chem. Phys.* **2**, 599 (1934).
50. L. Onsager, Initial recombination of ions, *Phys. Rev.* **54**, 554 (1938).
51. M. Pope and C.E. Swenberg, Electronic processes in organic solids, *Ann. Review Phys. Chem.* **35**, 613 (1984).
52. K.M. Hong and J. Noolandi, Solution of the time dependent Onsager problem, *J. Chem. Phys.* **69**, 5026 (1978).
53. H. Scher and S. Rackovsky, Theory of geminate recombination on a lattice, *J. Chem Phys.* **81**, 1994 (1984).
54. A. Mozumder, Influence of fractal geometry on geminate escape probability, mean recombination time, and homogenous reaction rates, *J. Chem Phys.* **92**, 1015 (1990).
55. M. Schott, Remarks on the process of carrier generation in electron-bombarded crystalline anthracene, *Mol. Cryst.* **5**, 229 (1969).
56. H. Sano and J.K. Baird, Brownian motion of reacting charged particles in ionizing tracks, *J. Chem. Phys.* **77**, 6236 (1982).